Available online at www.sciencedirect.com
ScienceDirect
Nuclear Medicine and Biology 36 (2009) 277–285
NUCLEAR MEDICINE — AND — BIOLOGY
www.elsevier.com/locate/nucmedbio

^{64}Cu-Labeled CB-TE2A and diamsar-conjugated RGD peptide analogs for targeting angiogenesis: comparison of their biological activity☆

Lihui Wei[a,1], Yunpeng Ye[a], Thaddeus J. Wadas[a], Jason S. Lewis[a,2], Michael J. Welch[a,b,d], Samuel Achilefu[a,b,c], Carolyn J. Anderson[a,b,c,d,*]

[a]*Mallinckrodt Institute of Radiology, Washington University School of Medicine, St. Louis, MO 63110, USA*
[b]*The Alvin J. Siteman Cancer Center, Washington University School of Medicine, St. Louis, MO 63110, USA*
[c]*Department of Biochemistry, Washington University School of Medicine, St. Louis, MO 63110, USA*
[d]*Department of Chemistry, Washington University School of Arts and Sciences, St. Louis, MO 63130, USA*

Received 29 August 2008; received in revised form 20 November 2008; accepted 11 December 2008

Abstract

Objectives: The $\alpha_v\beta_3$ integrin is a cell adhesion molecule known to be involved in stages of angiogenesis and metastasis. In this study, the chelators CB-TE2A and diamsar were conjugated to cyclic RGDyK and RGDfD and the biological properties of ^{64}Cu-labeled peptides were compared.

Methods: CB-TE2A-c(RGDyK) and diamsar-c(RGDfD) were labeled with ^{64}Cu in 0.1 M NH_4OAc (pH=8) at 95°C and 25°C, respectively. PET and biodistribution studies were carried out on M21 ($\alpha_v\beta_3$-positive) and M21L (α_v-negative) melanoma-bearing mice. Binding affinity of the Cu-chelator–RGD peptides to $\alpha_v\beta_3$ integrins was determined by a competitive binding affinity assay.

Results: Biological studies showed higher concentration of ^{64}Cu-CB-TE2A-c(RGDyK) in M21 tumor compared to M21L tumor at 1 and 4 h pi. Tumor concentration of ^{64}Cu-CB-TE2A-c(RGDyK) was higher than that of ^{64}Cu-diamsar-c(RGDfD). The difference is not due to differing binding affinities, since similar values were obtained for the agents. Compared to ^{64}Cu-diamsar-c(RGDfD), there is more rapid liver and blood clearance of ^{64}Cu-CB-TE2A-c(RGDyK), resulting in a lower liver and blood concentration at 24 h pi. Both ^{64}Cu-labeled RGD peptides show similar binding affinities to $\alpha_v\beta_3$. The differences in their biodistribution properties are likely related to different linkers, charges and lipophilicities. The M21 tumor is clearly visualized with ^{64}Cu-CB-TE2A-c(RGDyK) by microPET imaging. Administration of c(RGDyK) as a block significantly reduced the tumor concentration; however, the radioactivity background was also decreased by the blocking dose.

Conclusions: Both ^{64}Cu-CB-TE2A-c(RGDyK) and ^{64}Cu-diamsar-c(RGDfD) are potential candidates for imaging tumor angiogenesis. For diamsar-c(RGDfD), a linker may be needed between the Cu-chelator moiety and the RGD peptide to achieve optimal in vivo tumor concentration and clearance from nontarget organs.

Keywords: Copper-64; RGD; CB-TE2A; Diamsar

1. Introduction

Angiogenesis, the formation and differentiation of blood vessels, is required for both tumor growth and metastasis [1–3]. The angiogenic process depends on vascular endothelial cell migration and invasion, which are regulated by cell adhesion receptors. Integrins are a family of proteins that facilitate cellular adhesion and migration to extracellular matrix proteins found in intercellular spaces and basement membranes, and regulate cellular entry and withdrawal from the cell cycles [4–7]. Alpha v beta 3

☆ This work was partially supported by the National Cancer Institute (R24 CA86307 and R01 CA093375). Small animal PET imaging is supported by an NIH/NCI SAIRP grant (R24 CA86060) with additional support from the Small Animal Imaging Core of the Alvin J. Siteman Cancer Center at Washington University and Barnes-Jewish Hospital. The SAIC is supported by an NCI Cancer Center Support Grant P30 CA91842.

* Corresponding author. Mallinckrodt Institute of Radiology, Washington University School of Medicine, Campus Box 8225, St. Louis, MO 63110, USA. Tel.: +1 314 362 8427; fax: +1 314 362 9940.
E-mail address: andersoncj@wustl.edu (C.J. Anderson).
[1] Current affiliation: MDS Nordion, Ottawa, ON, Canada K2K 1X8.
[2] Current affiliation: Department of Radiology, Memorial Sloan-Kettering Cancer Center, New York, NY 10065, USA.

0969-8051/$ – see front matter © 2009 Elsevier Inc. All rights reserved.
doi:10.1016/j.nucmedbio.2008.12.008

($\alpha_v\beta_3$) integrin, one of the most extensively studied integrins, is highly expressed on activated endothelial and tumor cells during angiogenesis [8]. In contrast, expression of $\alpha_v\beta_3$ is weak in resting endothelial cells and most normal organ systems [4,9]. Therefore, $\alpha_v\beta_3$ integrin is a promising target for imaging tumor angiogenesis and for antiangiogenic therapy [10,11].

$\alpha_v\beta_3$ binds to the arginine-glycine-aspartate (RGD) amino acid sequence of extracellular matrix proteins such as vitronectin, fibrinogen or fibronectin [12,13]. In the past decade, various radiolabeled RGD peptide antagonists of $\alpha_v\beta_3$, have been developed as radiopharmaceuticals for single photon emission computed tomography and positron emission tomography (PET) imaging (see Refs. [14–16]). ^{64}Cu-Labeled RGD peptides are of particular interest. ^{64}Cu ($t_{1/2}$=12.7 h; 38% β^-, $E\beta^-_{max}$=573 keV; 19% β^+, $E\beta^+_{max}$=656 keV; 43% EC) is an attractive radionuclide for both PET imaging and targeted radiotherapy of cancer because of its decay characteristics [17,18], and because it can be produced at high specific activity on a small biomedical cyclotron [19].

RGD peptides can be radiolabeled with ^{64}Cu using a covalently bound bifunctional chelator. 1,4,7,10-Tetraazacyclododecane-1,4,7,10-tetraacetic acid (DOTA) and 1,4,8,11-tetraazacyclotetradecane-1,4,8,11-tetraacetic acid (TETA) have historically been used as bifunctional chelators for copper radionuclides [20–23]. We showed that ^{64}Cu-DOTA and ^{64}Cu-TETA complexes are moderately unstable in vivo due to the release of uncoordinated ^{64}Cu by decomposition in the blood or transchelation in the liver, causing high uptake in nontarget tissues [24,25]. Several new macrocyclic copper-chelating agents have been investigated for improving the in vivo stability of the ^{64}Cu complex. Novel bicyclic tetraazamacrocycle cross-bridged cyclam chelators have recently been developed for ^{64}Cu [26] that have shown significantly increased metal-chelate stability in vivo and, as a consequence, a reduced nontarget tissue accumulation [24,27]. ^{64}Cu-CB-TE2A-Tyr^3-Octreotate (where CB-TE2A is 4,11-bis(carboxymethyl)-1,4,8,11-tetraazabicyclo[6.6.2] hexadecane) (Fig. 1) has demonstrated improved blood, liver and kidney clearance compared with the analogous ^{64}Cu-TETA agent [27]. ^{64}Cu-CB-TE2A-ReCCMSH(Arg^{11}) also showed greatly improved liver and blood clearance as well as higher tumor-to-nontarget tissue ratios compared with ^{64}Cu-DOTA-ReCCMSH(Arg^{11}) [28].

A new class of cage-type hexaazamacrobicyclic sarcophagine (Sar) chelators and derivatives has also been developed as stable Cu chelates [29–33]. A recently developed bifunctional version of the Sar chelator — SarAr — has been conjugated to antibodies and the resulting SarAr immunoconjugates have been radiolabeled with ^{64}Cu. ^{64}Cu-Labeled SarAr conjugated anti-GD2 monoclonal antibody (mAb) 14.G2a and its chimeric derivative, ch14.18, were shown to have high specific activity, antigen binding and in vivo target specificity to neuroblastoma and melanoma, with minimal uptake in normal tissues [34]. SarAr has also been conjugated to the well-characterized B72.3 antibody and its fragments, and ^{64}Cu-SarAr immunoconjugates maintain their specificity for the target and are stable in vivo [35].

Both cross-bridged and Sar chelate systems have shown significant metal-chelate stability and, consequently, low nontarget tissue accumulation. The objective of this research was to compare the in vivo and in vitro biological activities of the cross-bridged and Sar chelator using RGD peptide analogs as targeting molecules.

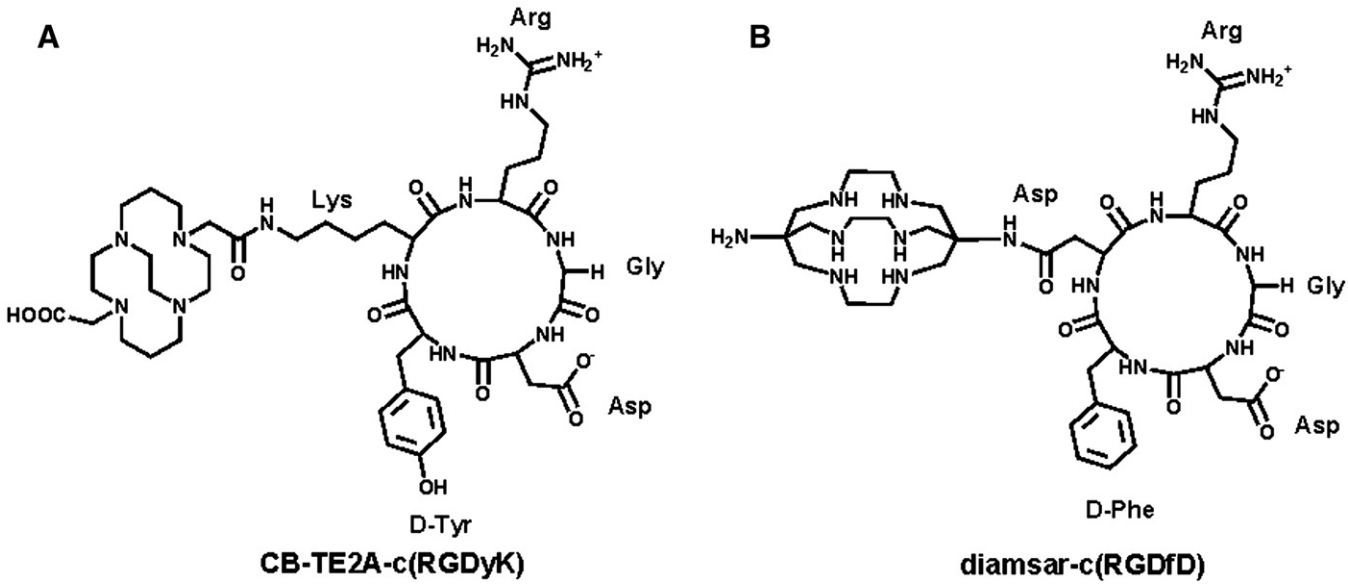

Fig. 1. (A) Structure of CB-TE2A-c(RGDyK) and (B) structure of diamsar-c(RGDfD).

2. Materials and methods

2.1. General

All chemicals unless otherwise stated were purchased from Sigma-Aldrich Chemical Co. (St. Louis, MO, USA). Water was distilled and then deionized (18 MΩ/cm^2) by passing through a Milli-Q water filtration system (Millipore Corp., Milford, MA, USA). ^{64}Cu was produced on a CS-15 biomedical cyclotron at Washington University School of Medicine according to published procedure [19]. Radioactivity was counted with a Beckman Gamma 8000 counter containing a NaI crystal (Beckman Instruments, Inc., Irvine, CA, USA). Radio-TLC detection was accomplished using a BIOSCAN AR2000 Imaging Scanner (Washington, DC). Analytical reversed-phase high-performance liquid chromatography (HPLC) was performed on a 600E chromatography system (Waters) with a 996 photodiode array detector (Waters) and an Ortec Model 661 radioactivity detector (EG&G Instruments, Oak Ridge, TN, USA). Electrospray mass spectrometry was accomplished using a Micromass ZQ (Waters).

2.2. Synthesis of CB-TE2A-c(RGDyK)

The cyclic peptide (Fig. 1A) was prepared in three steps consisting of solid-phase peptide synthesis, intramolecular cyclization in solution, and conjugation of peptide with CB-TE2A, as described previously [36]. The crude product was purified by HPLC and identified by electrospray mass spectrometry. The observed *m/z* for $[MH]^+$ and $[MH_2]^{2+}$ in electrospray mass spectrometry was 944.37 and 472.77, respectively. Unconjugated c(RGDyK) for the integrin-binding assays and blocking studies in mice was purchased from CS Bio (Menlo Park, CA, USA).

2.3. Synthesis of diamsar-c(RGDfD)

Diamsar was synthesized following literature procedures [29,32]. Briefly, cobalt(III) complex of the diamine derivative of the Sar compound (diamsar) was prepared by template synthesis based on tris(ethane-1,2-diamine)cobalt (III). Co(III)–diamsar complex was reduced to its Co(II) form to enable the removal of the diamsar ligand. The reduction reaction was performed in hot aqueous solution containing excess cyanide ion.

Diamsar-c(RGDfD) (Fig. 1B) was synthesized by a similar procedure as that of CB-TE2A-c(RGDyK). Briefly, the orthogonally protected linear peptide [H-Asp(OBut)-DPhe-Asp(ODmab)-Arg(Pbf)-Gly-OH] was prepared from a H-Gly-2-chlorotrityl resin and cleaved with 1% TFA in dichloromethane. The cyclization was realized in the presence of PyBOP, *N*-hydroxybenzotriazole (HOBT) and diisopropylethylamine in *N,N*-dimethylformamide/dichloromethane. The ODmab group was deprotected with 2% hydrazine in aqueous acetonitrile. Diamsar was conjugated to the carboxylic acid group of aspartic acid of the peptide in the presence of diisopropylcarbodiimide and HOBT in anhydrous *N,N*-dimethylformamide. All side-chain–protecting groups were removed with 95% aqueous TFA solution, and the crude product was purified by HPLC and identified by electrospray mass spectrometry. The observed *m/z* for $[MH_2]^{2+}$ in electrospray mass spectrometry was 444.3.

2.4. ^{64}Cu Radiolabeling

CB-TE2A-c(RGDyK) was radiolabeled with ^{64}Cu according to the method reported previously for radiolabeling of CB-TE2A conjugates [27,28,36]. Briefly, $^{64}CuCl_2$ was added to CB-TE2A-c(RGDyK) in 0.1 M NH_4OAc (pH 8) and heated at 95°C for 1 h. Radiochemical purity was >95% as confirmed by both radio-HPLC (99% A to 70% A in 15 min, 1 ml/min; A: 0.1% TFA in H_2O, B: 0.1% TFA in acetonitrile; C-18 monomeric column [Vydac], 3 mm, 4.6×100 mm) and radio-TLC [Whatman MKC18F reversed-phase plates with 10% ammonium acetate/methanol (30:70) as the mobile phase].

Diamsar-c(RGDfD) was labeled with ^{64}Cu under milder reaction conditions. $^{64}CuCl_2$ was added to diamsar-c (RGDfD) solution in 0.1 M NH_4OAc (pH 8), and the reaction mixture was incubated at 25°C for 1 h. Radio-HPLC and radio-TLC (conditions same as above) assessment showed that the radiochemical purity was >95%.

2.5. In vitro binding assay

The binding affinity of Cu-CB-TE2A-c(RGDyK) and Cu-diamsar-c(RGDfD) for $\alpha_v\beta_3$ integrin was estimated using previously reported methods [37]. Briefly, vitronectin (Chemicon, Temecula, CA) (630 μg/ml) was biotinylated with *N*-hydroxysuccinimide biotin (1.27 μg/ml; 2 h at room temperature) prior to dialysis into PBS, pH 7.4. Integrin $\alpha_v\beta_3$ (EMD Bioscience, San Diego, CA, USA) [1 μg/ml in 20 mM Tris, pH 7.4, 150 mM NaCl, 2 mM $CaCl_2$, 1 mM $MgCl_2$, 1 mM $MnCl_2$ (coating buffer)] was layered onto 96-well plates (Nunc Immuno Plate with MaxiSorp) (1 h at 4°C). Plates were then blocked (1 h at 4°C) with BSA (3% in coating buffer). After washing twice with binding buffer (0.1% BSA in coating buffer), biotinylated vitronectin (14 nM) and serially diluted peptides were allowed to bind to the integrins (3 h at 37°C). Following washing (three times in binding buffer), bound biotinylated vitronectin was detected by binding ExtrAvidin-Alkaline Phosphatase (Sigma) (1/35,000 dilution, 1 h at RT) using *p*-Nitrophenyl Phosphate Liquid Substrate System (Sigma) as the chromogen. Assays were performed in triplicate. Nonlinear regression was used to fit binding curves and calculate IC_{50} values (GraphPad Prism 4.0, San Diego, CA, USA).

2.6. Biodistribution studies

All animal experiments were conducted in compliance with the Guidelines for the Care and Use of Research Animals established by Washington University's Animal Studies Committee. Biodistribution studies were carried out on 24- to 29-g male Nu/Nu mice (Charles River

Laboratories, Wilmington, MA, USA) that had been implanted with cultured M21 and M21L human melanoma cells. Due to the lack of the α_v subunit, M21L cells have different growth characteristics compared to M21 cells. To obtained comparable tumor xenografts, 5×10^6 M21 and 2×10^7 M21L cells were injected subcutaneously into the left and right thigh of the mice, respectively [38]. Tumors were allowed to grow for 21 days, at which time the animals received ~10 μCi of ^{64}Cu-CB-TE2A-c(RGDyK) or ^{64}Cu-diamsar-c(RGDfD) in 100 μl of saline via lateral tail vein injection. For each peptide, four groups were examined at four time points [n=5 per group at 1, 2, 4 and 24 h postinjection (pi)]. In all studies following euthanasia, tissues and organs of interest were removed and weighed, and the radioactivity was measured in a γ-counter. The percent doses per gram (%ID/g) were then calculated by comparison to known standards.

2.7. Small animal PET studies

Whole-body small animal PET imaging was performed on a microPET Focus scanner (Concorde Microsystems, Knoxville, TN, USA) [39]. Imaging studies were carried out on Nu/Nu mice bearing 21-day M21 and M21L human melanoma tumors. The mice were injected via the tail vein with ^{64}Cu-CB-TE2A-c(RGDyK) (150 μCi). At 1, 2 4 and 24 h after injection, the mice were anesthetized with 1% to 2% isoflurane, positioned supine, immobilized and imaged side by side with mice that had been treated with cyclic RGDyK as a block (~15 mg/kg). Ten-minute static data sets were collected at each time point.

2.8. Statistical methods

All of the data are presented as mean±S.D. For statistical classification, a Student's t test was performed using GraphPad PRISM (San Diego, CA, USA). Differences at the 95% confidence level (P<.05) were considered significant.

3. Results

3.1. Synthesis of CB-TE2A-c(RGDyK) and diamsar-c (RGDfD)

The carboxylic acid arm of the cross-bridged CB-TE2A was conjugated to the ε-amine of the lysine group of cyclic pentapeptide RGDyK, while the amine group of diamsar was coupled to the carboxylic acid of the aspartic acid group of cyclic RGDfD. The conjugated peptides were prepared in three steps. First, the linear peptides were synthesized by solid-phase peptide synthesis using Fmoc chemistry, followed by intramolecular cyclization to form cyclic pentapeptides c(RGDyK) and c(RGDfD), and conjugation of the peptides with chelates CB-TE2A and diamsar. The conjugated peptides were purified by RP-HPLC and identified by positive ion electrospray mass spectrometry.

Table 1
Affinity of Cu(II)-CB-TE2A-c(RGDyK) [30] and Cu(II)-DiamSar-c (RGDfD) for integrin $\alpha_v\beta_3$ as determined in heterologous competitive binding assay using biotinylated vitronectin [c(RGDyK) [30] was used as a control]

Compound	IC_{50} (nM)	95% confidence intervals (nM)
Cu(II)-CBTE2A-c(RGDyK)	6.0	3.7–9.6
Cu(II)-DiamSar-c(RGDfD)	4.8	3.9–5.8
c(RGDyK)	3.7	2.7–5.0

Table 2
Biodistribution of ^{64}Cu-DiamSar-c(RGDfD) and ^{64}Cu-CBTE2A-c(RGDyK) (%ID/g±SD, n=5) at 1, 2, 4 and 24 h pi in Nu/Nu mice implanted bilaterally with 21-day M21 and M21L melanoma tumors

Tissue	1 h	2 h	4 h	24 h
^{64}Cu-DiamSar-c(RGDfD)				
Blood	0.60±0.31	0.14±0.04	0.06±0.02	0.08±0.01
Lung	1.59±0.29	1.05±0.13	0.90±0.33	0.63±0.09
Liver	2.33±0.76	2.63±0.53	2.17±0.64	2.24±0.41
Spleen	1.08±0.34	1.11±0.19	0.87±0.25	0.77±0.17
Kidney	5.58±1.62	3.78±0.29	3.17±0.96	2.36±0.35
Muscle	0.81±0.36	0.19±0.03	0.13±0.04	0.13±0.03
Heart	0.56±0.09	0.37±0.13	0.23±0.09	0.26±0.03
Bone	2.28±1.44	0.46±0.22	0.23±0.12	0.29±0.07
M21	1.51±0.53	0.79±0.22	0.52±0.29	0.47±0.10
M21L	1.16±0.47	0.65±0.08	0.39±0.14	0.32±0.08
Tumor (M21)/blood	4.36±0.68	6.11±1.85	9.50±1.51	6.31±1.06
^{64}Cu-CBTE2A-c(RGDyK)				
Blood	0.85±0.46	0.27±0.13	0.13±0.11	0.02±0.01
Lung	2.38±0.86	1.64±0.40	1.06±0.05	0.41±0.07
Liver	3.86±1.98	2.53±0.89	1.92±0.29	0.84±0.17
Spleen	2.17±0.60	1.90±0.78	1.58±0.24	1.66±1.15
Kidney	5.96±1.20	5.18±1.67	3.96±0.53	2.10±0.86
Muscle	1.15±0.78	0.37±0.09	0.47±0.18	0.15±0.04
Heart	1.22±0.48	0.66±0.30	0.34±0.04	0.23±0.07
Bone	3.80±1.15	0.76±0.17	0.50±0.08	0.59±0.48
M21	2.99±0.90	1.68±0.58	1.66±0.80	0.70±0.17
M21L	1.76±0.43	1.40±0.54	0.84±0.41	0.80±0.35
Tumor (M21)/blood	4.51±2.89	6.46±1.30	18.34±5.10	26.31±3.24

3.2. Radiolabeling of CB-TE2A-c(RGDyK) and diamsar-c (RGDfD) with ^{64}Cu

CB-TE2A-c(RGDyK) was successfully labeled with ^{64}Cu in 0.1 M ammonium acetate buffer (pH=8) at 95°C for 1 h. ^{64}Cu labeling of diamsar-c(RGDfD) was performed in the same reaction buffer and same reaction time but at lower temperature (25°C). Without a purification procedure, we were able to achieve radiochemical purities of >95% for both radiolabeled peptides. For the purpose of direct comparison of their biological properties, the specific activities of the two ^{64}Cu-labeled peptides were controlled to be similar (~1 mCi/μg corresponding to ~1000 mCi/μmol).

3.3. In vitro competitive binding assay

The nonradioactive Cu complexes of the chelator-conjugated RGD peptides were synthesized using similar

procedures as those for the ^{64}Cu radiolabeling. Their binding affinity to $\alpha_v\beta_3$ integrin was determined by a competitive binding affinity assay using biotinylated vitronectin and target ligands. IC_{50} values (the concentration of peptide/antagonist required to inhibit 50% of vitronectin binding to integrin) of the two compounds are very similar, indicating comparable binding affinity to $\alpha_v\beta_3$ integrin (Table 1).

3.4. Biodistribution studies

Biodistribution studies for ^{64}Cu-CB-TE2A-c(RGDyK) and ^{64}Cu-diamsar-c(RGDfD) were carried out in nude mice using the $\alpha_v\beta_3$-positive xenotransplanted human melanoma M21 model [37,40]. M21L cells have low α_v expression and were therefore selected as the negative control [40,41]. M21 and M21L cells were implanted into the left and right thigh of the mice, respectively. Table 2 presents the biodistribution data at 1, 2, 4 and 24 h after injection of 10 μCi of ^{64}Cu-diamsar-c(RGDfD) and ^{64}Cu-CB-TE2A-c(RGDyK).

Biodistribution data showed higher concentration in M21 tumor compared to M21L tumor for ^{64}Cu-CB-TE2A-c (RGDyK) at 1 and 4 h pi [e.g., at 1 h pi, 2.99±0.90 (M21) vs. 1.76±0.43 %ID/g (M21L), $P\approx.02$; at 4 h pi, 1.66±0.8 (M21) vs. 0.84±0.41 %ID/g (M21L), $P<.04$]. For ^{64}Cu-diamsar-c(RGDfD), the M21 tumor concentration was slightly higher than M21L; however, statistical analysis showed that M21 and M21L concentrations were not significantly different [P=NS (not significant)] at 1, 2 and 4 h pi. Only at 24 h pi is there a significant difference in the uptake between the two cell lines ($P\approx.03$) (Table 2). The concentration of ^{64}Cu-CB-TE2A-c(RGDyK) in M21 tumor was higher than that of ^{64}Cu-diamsar-c(RGDfD) at all time points (e.g., at 1 h pi, ^{64}Cu-CB-TE2A-c(RGDyK): 2.99±0.90 vs. ^{64}Cu-diamsar-c(RGDfD): 1.51±0.53 %ID/g, $P<.01$; at 4 h pi, ^{64}Cu-CB-TE2A-c(RGDyK): 1.66±0.80 vs. ^{64}Cu-diamsar-c(RGDfD): 0.52±0.29 %ID/g, $P<.02$) (Table 2 and Fig. 2).

Table 2 and Fig. 2 indicate that the radioactivity in the liver and blood was higher for ^{64}Cu-CB-TE2A-c(RGDyK) than for ^{64}Cu-diamsar-c(RGDfD) at 1 h pi [liver uptake: ^{64}Cu-CB-TE2A-c(RGDyK): 3.86±1.98 vs. ^{64}Cu-diamsar-c(RGDfD): 2.33±0.76 %ID/g, $P<.05$; blood uptake: ^{64}Cu-CB-TE2A-c

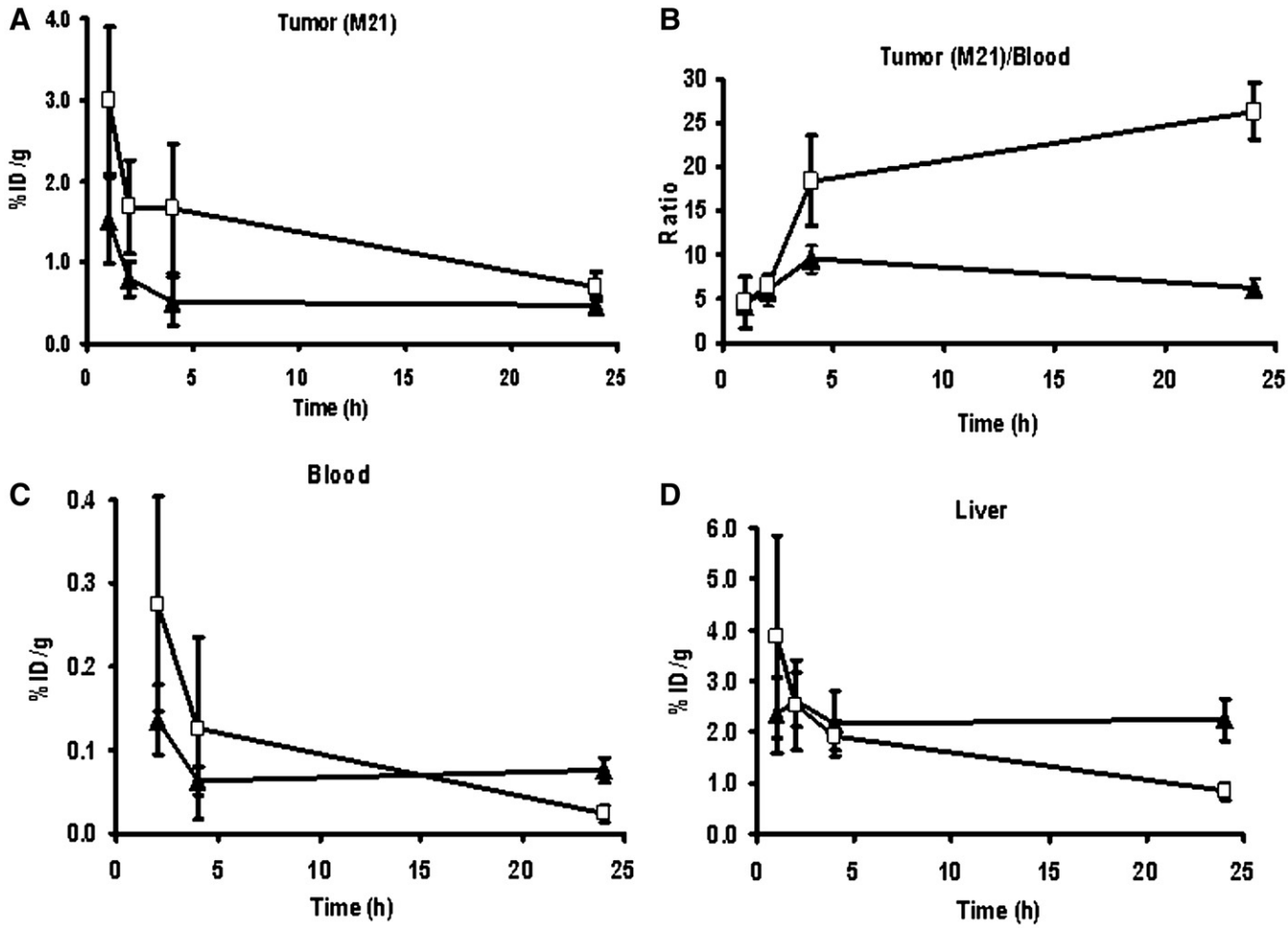

Fig. 2. Comparison of biodistribution of ^{64}Cu-CB-TE2A-c(RGDyK) (10 μCi, n=4; □) and ^{64}Cu-diamsar-c(RGDfD) (10 μCi, n=4; ▲) in M21 and M21L tumor-bearing Nu/Nu mice. Data are presented as %ID/g±S.D. Note the difference in y-axis scales. (A) M21 and M21L tumor uptakes. (B) Tumor/blood ratios. (C) Blood clearance. (D) Liver clearance.

(RGDyK): 0.85±0.46 vs. ^{64}Cu-diamsar-c(RGDfD): 0.60±0.31 %ID/g, *P*=NS]. However, compared to ^{64}Cu-diamsar-c (RGDfD), there is more rapid liver and blood clearance of ^{64}Cu-CB-TE2A-c(RGDyK), resulting in a lower liver and blood concentration at 24 h pi. For example, the liver uptake of ^{64}Cu-CB-TE2A-c(RGDyK) at 24 h pi had fallen to ~20% of the 1-h uptake (1 h pi: 3.86±1.98 vs. 24 h pi: 0.84±0.17 %ID/g, *P*<.02), while for ^{64}Cu-diamsar-c(RGDfD), the radioactivity in liver did not change significantly from 1 to 24 h pi (1 h pi: 2.33±0.76 vs. 24 h pi: 2.24±0.41 %ID/g, *P*=NS). The ^{64}Cu-CB-TE2A-c(RGDyK) activity in the blood was reduced by 98% from 1 to 24 h pi compared with an 86% reduction for ^{64}Cu-diamsar-c(RGDfD) activity over the same period [^{64}Cu-CB-TE2A-c(RGDyK): 0.85±0.46 (1 h pi) vs. 0.02±0.01 % ID/g (24 h pi), *P*<.01; ^{64}Cu-diamsar-c(RGDfD): 0.60±0.31 (1 h pi) vs. 0.08±0.01 %ID/g (24 h pi), *P*<.02]. Because of the higher tumor concentration and faster blood clearance, the tumor (M21)-to-blood ratio of ^{64}Cu-CB-TE2A-c (RGDyK) is higher than that of ^{64}Cu-diamsar-c(RGDfD) at later time points. Table 2 and Fig. 2 show that the tumor/blood ratio of ^{64}Cu-CB-TE2A-c(RGDyK) is similar to ^{64}Cu-diamsar-c(RGDfD) at 1 and 2 h pi but is significantly higher than ^{64}Cu-diamsar-c(RGDfD) at 4 and 24 h pi [at 4 h pi, ^{64}Cu-CB-TE2A-c(RGDyK): 18.34±5.10 vs. ^{64}Cu-diamsar-c (RGDfD): 9.50±1.51 %ID/g, *P*<.05; at 24 h pi; ^{64}Cu-CB-TE2A-c(RGDyK): 26.31±3.24 vs. ^{64}Cu-diamsar-c(RGDfD): 6.31±1.04 %ID/g, *P*<.05].

3.5. Small animal PET studies

Because of its higher tumor concentration, ^{64}Cu-CB-TE2A-c(RGDyK) was chosen for a small animal PET imaging study. Small animal PET images were obtained with nude mice bearing 21-day M21 and M21L human melanoma tumors. Fig. 3 shows the projection images of the mice at 1 h after injection of 150 μCi of ^{64}Cu-CB-TE2A-c (RGDyK). The image of the control mice on the right side demonstrated that the M21 tumor was clearly visualized, while much lower activity accumulation was found in M21L tumor, which is consistent with the biodistribution data. The mouse on the left side was preinjected with 15 mg of c (RGDyK) per kilogram of body weight as a block. The results show that the block dramatically reduced the radioactivity accumulation in the tumor by such an extent that very little activity can be seen in the tumor. However, Fig. 3 shows that treatment with c(RGDyK) also reduced uptake in other tissues such as the kidney, resulting in lower radioactivity concentrations in both tumor and the background for the c (RGDyK)-treated mouse.

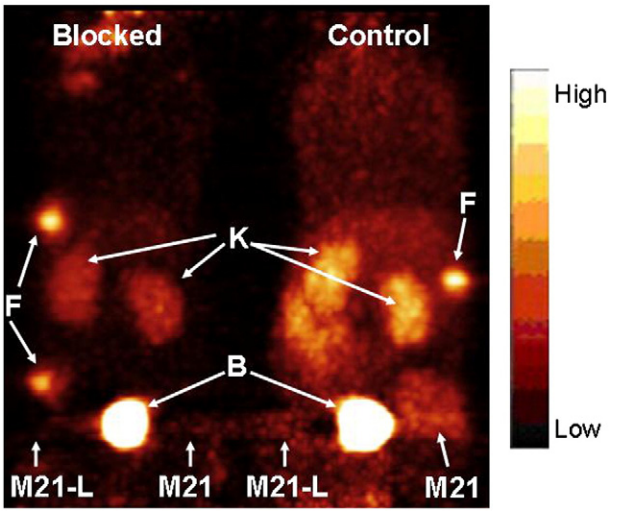

Fig. 3. MicroPET projection images of Nu/Nu mice implanted with M21 and M21L tumors at 1 h after tail vein injection of 150 μCi of ^{64}Cu-CB-TE2A-c (RGDyK). A mouse that received blockade (left) was co-imaged with a mouse that did not receive blockade (right). The blockade mouse received 15 mg/kg of c(RGDyK). The PET images show that the administration of a blockade dose substantially reduces M21 tumor uptake of the agent by such an extent that the tumor is difficult to delineate. (K=kidney, B=bladder, F=fiducial marker.)

4. Discussion

The procedures for the conjugation of both chelating groups with the RGD peptides were similar. Although CB-TE2A possesses two carboxylic acid functions, previous studies demonstrated the selective conjugation of partially protected c(RGDyK) with only one of the acid groups [27,28,36]. Unlike CB-TE2A, however, diamsar contains eight amino acid groups that can potentially react with the peptide. To prepare diamsar-c(RGDfD), we used orthogonally protected RGD peptide, c[R(Pbf)GD(OBut)fD] and reaction conditions that favor conjugation of only one of the diamsar's primary amines with the unprotected aspartic acid group of the peptide. HPLC purification gave a major peak that was identified by both ES-MS and analytical HPLC as the mono-conjugate. The synergistic effects of mild reaction conditions and higher reactivity of the primary relative to the secondary amines because of steric factors further support the structure depicted in Fig. 1.

To facilitate ^{64}Cu labeling, antibodies or peptides have been historically conjugated to one of the bifunctional chelators, DOTA or TETA. Biodistribution and metabolism studies of ^{64}Cu-labeled DOTA/TETA monoclonal antibody or peptide conjugates have demonstrated significant dissociation of the ^{64}Cu from the bifunctional chelator resulting in transchelation to liver superoxide dismutase and other proteins [24,27,42–44]. ^{64}Cu-labeled DOTA/TETA conjugates often show poor blood and liver clearance, high uptake in some nontarget organs and increased background radioactivity levels, resulting in reduced imaging sensitivity, poor image quality and radiation toxicity [45,46].

A series of copper(II) cross-bridged cyclam complexes have been synthesized and characterized, and have demonstrated improved kinetic stability compared with TETA and DOTA complexes [26,47]. The biodistribution of four ^{64}Cu-labeled cross-bridged cyclam complexes has been evaluated, and it was found that ^{64}Cu-CB-TE2A had the most improved

blood, liver and kidney clearance [25]. Another type of Cu chelator has been developed based on hexa-aza macrobicyclic sarcophagine (Sar) cage [29,31,48]. The cage-type ligands, designed with the additional linking strand incorporating two nitrogen atoms, form a three-dimensional "cage" around the Cu^{2+} ion which leads to an increased thermodynamic and kinetic stability [49,50]. In this study, we intended to compare the biological properties of the cross-bridged and Sar chelators using RGD peptide analogs as targeting molecules.

One of the selective $\alpha_v\beta_3$ antagonists is a cyclic pentapeptide c(RGDfV) with IC_{50} values in the lower nanomolar range [51]. Additional studies showed that, besides the essential RGD sequence, a hydrophobic amino acid in Position 4 increases the affinity, whereas the amino acid in Position 5 has no effect on the affinity [52]. We selected two cyclic RGD peptides, c(RGDyK) and c(RGDfD), both of which have hydrophobic amino acids (tyrosine or phenylalanine, respectively) in Position 4. Lysine group in Position 5 in c(RGDyK) offers an ε-amine group which can be coupled to the carboxylic acid group of the chelate CB-TE2A. For c(RGDfD), the aspartic acid group was chosen for Position 5 to facilitate the conjugation with the amine group of the diamsar chelator. The chelator-conjugated peptides were synthesized by similar procedures. The linear peptides were first prepared by Fmoc solid-phase peptide synthesis technique, followed by intramolecular cyclization and finally conjugation of the peptides with the chelators.

CB-TE2A-c(RGDyK) and diamsar-c(RGDfD) were radiolabeled with ^{64}Cu in the same basic reaction buffer (0.1 M NH_4OAc, pH 8). Radiolabeling of CB-TE2A-c(RGDyK) was performed at high temperature (95°C), while milder temperature (25°C) was required for the radiolabeling of diamsar-c(RGDfD). It was reported that cage-type chelate Sar and its derivative, SarAr, can be labeled with ^{64}Cu over a pH range of 4–9 [30,31], and SarAr immunoconjugates were radiolabeled with ^{64}Cu at pH 5 [34,35]. Both SarAr and SarAr-conjugated antibodies could be rapidly radiolabeled (<10 min) at room temperature [30,31,34,35]. However, in our study, by monitoring the labeling reaction with radio-TLC, we found that the ^{64}Cu labeling of diamsar-c(RGDfD) was not completed within 30 min, and 1 h is the optimal reaction time to ensure the highest radiolabeling yield. The ^{64}Cu labeling of diamsar-c(RGDfD) at pH 6 and 8 showed similar reaction rates. However, a complete investigation of the labeling conditions, such as other pH values, different buffers and molar ratios of diamsar-c(RGDfD) to ^{64}Cu, was not performed. Therefore, the labeling conditions may not be optimized. Moreover, the chelator used in previously reported SarAr-conjugated antibody B72.3 [35] contains a benzyl amine linker, while in diamsar-c(RGDfD) the Sar chelating moiety is closer to the RGD peptide. Also, the peptide c(RGDfD) was attached to the chelator diamsar by a short aspartic acid linker. The short distance between diamsar and c(RGDfD) may impact the kinetics of radiolabeling.

For in vivo evaluation, we chose the human xenograft M21 and M21L melanoma model. The M21 cells express $\alpha_v\beta_3$ [37,40], while the M21L cell line is a stable variant cell line of M21 failing to transcribe the α_v gene and therefore serves as a negative control [41]. At 1 and 4 h postinjection, the M21 tumor concentration is higher than M21L concentration for ^{64}Cu-CB-TE2A-c(RGDyK). ^{99m}Tc-DKCK-c(RGDfK) was studied previously using the same M21/M21L tumor model, and it was reported that the M21 tumor accumulation decreases from 1.91±0.24 %ID/g at 30 min pi to 1.10±0.22 %ID/g at 4 h pi In contrast, the M21L tumor uptake ranges from 0.74±0.06 %ID/g at 30 min pi to 0.31±0.09 %ID/g at 4 h pi [38]. The magnitude of the tumor uptake values of ^{64}Cu-labeled RGD peptides in this study as shown in Table 2 is in the same range as the M21 and M21L tumor uptakes of ^{99m}Tc-DKCK-c(RGDfK).

Small animal PET imaging also showed higher radioactivity concentration in the M21 tumor compared to M21L tumor for ^{64}Cu-CB-TE2A-c(RGDyK), which is consistent with the biodistribution data. The blocking study showed that adding excess RGD peptide c(RGDyK) significantly decreased the tumor concentration, as well as reduced the uptake in other organs such as kidney. Similar multiorgan blocking has been reported for a tetrameric RGD peptide ^{64}Cu-DOTA-E{E[c(RGDfK)]$_2$}$_2$ in the U87MG tumor model [53] and also for ^{64}Cu-CB-TE2A-c(RGDyK) in the parathyroid hormone mouse model [36]. This is not unexpected, as it is well known that RGD peptides do show low-level affinity for other integrins [54]. Also, nontarget organs express a low amount of integrin $\alpha_v\beta_3$ by Western blot analysis [53].

The biodistribution study demonstrated that, compared to ^{64}Cu-diamsar-c(RGDfD), ^{64}Cu-CB-TE2A-c(RGDyK) showed higher tumor uptake, faster liver and blood clearance, and higher tumor-to-blood ratio at 4 and 24 h pi, indicating superior properties of ^{64}Cu-CB-TE2A-c(RGDyK). The in vitro binding assay showed similar $\alpha_v\beta_3$ binding affinity for ^{64}Cu-CB-TE2A-c(RGDyK) and ^{64}Cu-diamsar-c(RGDfD), which proved that the binding affinity does not contribute to the differences of their biodistribution properties. The chelator conjugation seems to have minimal impact on the integrin binding affinity of the RGD peptides. Similar results were reported previously for DOTA-conjugated dimeric and tetrameric RGD peptides E[c(RGDfK)]$_2$ and E{E[c(RGDfK)]$_2$}$_2$ [53].

The differences in the biodistribution data of the two ^{64}Cu-labeled RGD peptides are likely related to their molecular structures. Cu-CB-TE2A-c(RGDyK) has a longer lysine linker, while Cu-diamsar-c(RGDfD) has a shorter aspartic acid linker. Moreover, different charges and lipophilicities may also cause their pharmacokinetic differences. The ligand donors for ^{64}Cu-diamsar-c(RGDfD) are amines which make the labeled peptide more positively charged compared to ^{64}Cu-CB-TE2A-c(RGDyK) whose ligand donors are with a combination of amines, amide and carboxylic acid moieties. ^{64}Cu-CB-

TE2A-c(RGDyK) is more hydrophilic than ^{64}Cu-diamsar-c (RGDfD) with tyrosine in Position 4 instead of phenylalanine. A future direction is to modify the structure of the Sar-RGD peptide in order to directly compare CB-TE2A and Sar-conjugated RGD peptides. For example, a successful synthesis of the carboxylic acid derivatives of the Sar ligand would allow coupling of the acid group with the ε-amine of lysine to isolate diamsar-c(RGDyK). Alternatively, utilizing the SarAr bifunctional chelator that has been evaluated for radiolabeling ^{64}Cu-labeled mAbs [27] may provide more optimal results.

5. Conclusions

We successfully synthesized and purified CB-TE2A-c (RGDyK) and diamsar-c(RGDfD), and radiolabeled the peptides with ^{64}Cu. The tumor concentration of ^{64}Cu-CB-TE2A-c(RGDyK) in the $\alpha_v\beta_3$-positive M21 tumor is higher than that in the negative control M21L tumor at 1 and 4 h postinjection. The $\alpha_v\beta_3$ binding affinities of the two Cu-chelator-RGD peptides are similar. Compared to ^{64}Cu-diamsar-c(RGDfD), ^{64}Cu-CB-TE2A-c(RGDyK) is a superior compound for $\alpha_v\beta_3$ integrin targeting with higher tumor uptake, faster liver and blood clearance, and a higher tumor/blood ratio. For diamsar-c(RGDfD), a suitable linker may be needed between the Cu-chelate moiety and the cyclic RGD peptide to achieve optimal in vivo stability and tumor uptake.

Acknowledgments

We are very grateful for the technical assistance of Dawn Werner, Terry Sharp, Lori Strong, Nicole Fettig, Margaret Morris, Amanda Roth, Ann Stroncek and Jerrel Rutlin. We further wish to thank Dr. Gary R. Weisman and Dr. Edward H. Wong at the University of New Hampshire for supplying the chelator CB-TE2A.

References

[1] Folkman J. Tumor angiogenesis. Adv Cancer Res 1985;43:175–203.
[2] Folkman J. Role of angiogenesis in tumor growth and metastasis. Semin Oncol 2002;29:15–8.
[3] Brower V. Tumor angiogenesis—new drugs on the block. Nat Biotechnol 1999;17:963–8.
[4] Brooks PC, Clark RAF, Cheresh DA. Requirement of vascular integrin alpha v beta 3 for angiogenesis. Science 1994;264:569–71.
[5] Hwang R, Varner J. The role of integrins in tumor angiogenesis. Hematol Oncol Clin North Am 2004;18:991–1006.
[6] Jin H, Varner J. Integrins: roles in cancer development and as treatment targets. Br J Cancer 2004;90:561–5.
[7] Kumar CC. Integrin alpha v beta 3 as a therapeutic target for blocking tumor-induced angiogenesis. Curr Drug Targets 2003;4:123–31.
[8] Brooks PC, Montgomery AMP, Rosenfeld M, Reisfeld RA, Hu T. Integrin αvβ3 antagonists promote tumor-regression by inducing apoptosis of angiogenic blood vessels. Cell 1994;79:1157.
[9] Eliceiri BP, Cheresh DA. The role of alpha v integrins during angiogenesis: insights into potential mechanisms of action and clinical development. J Clin Invest 1999;103:1227–30.
[10] Tucker GC. Alpha v integrin inhibitors and cancer therapy. Curr Opin Investig Drugs 2003;4:722–31.
[11] McQuade P, Knight LC. Radiopharmaceuticals for targeting the angiogenesis marker alpha(v)beta(3). Q J Nucl Med 2003;47:209–20.
[12] Ruoslahti E. RGD and other recognition sequences for integrins. Annu Rev Cell Dev Biol 1996;12:697–715.
[13] Ruoslahti E, Pierschbacher MD. Arg-Gly-Asp — a versatile cell recognition signal. Cell 1986;44:517–8.
[14] Haubner R, Wester HJ. Radiolabeled tracers for imaging of tumor angiogenesis and evaluation of anti-angiogenic therapies. Curr Pharm Des 2004;10:1439–55.
[15] Haubner RH, Wester HJ, Weber WA, Schwaiger M. Radiotracer-based strategies to image angiogenesis. Q J Nucl Med 2003;47:189–99.
[16] Liu S. Radiolabeled multimeric cyclic RGD peptides as integrin αvβ3 targeted radiotracers for tumor imaging. Mol Pharmacol 2006;3:472–87.
[17] Qaim SM. Decay data and production yields of some non-standard positron emitters used in PET. Q J Nucl Med Mol Imaging 2008;52:111–20.
[18] Qaim SM, Bisinger T, Hilgers K, Nayak D, Coenen HH. Positron emission intensities in the decay of 64Cu, 76Br and 124I. Radiochim Acta 2007;95:67–73.
[19] McCarthy DW, Shefer RE, Klinkowstein RE, Bass LA, Margeneau WH, Cutler CS, et al. Efficient production of high specific activity 64Cu using a biomedical cyclotron. Nucl Med Biol 1997;24:35–43.
[20] Moi MK, Meares CF, McCall MJ, Cole WC, Denardo SJ. Copper-chelates as probes of biological-systems — stable copper-complexes with a macrocyclic bifunctional chelating agent. Anal Biochem 1985;148:249–53.
[21] Anderson CJ, Connett JM, Schwarz SW, Rocque PA, Guo LW, Philpott GW, et al. Copper-64-labeled antibodies for PET imaging. J Nucl Med 1992;33:1685–91.
[22] Jones-Wilson TM, Deal KA, Anderson CJ, McCarthy DW, Kovacs Z, Motekaitis RJ, et al. The in vivo behavior of copper-64-labeled azamacrocyclic complexes. Nucl Med Biol 1998;25:523–30.
[23] Anderson CJ, Dehdashti F, Cutler PD, Schwarz SW, Laforest R, Bass LA, et al. Cu-64-TETA-Octreotide as a PET imaging agent for patients with neuroendocrine tumors. J Nucl Med 2001;42:213–21.
[24] Boswell CA, Sun X, Niu W, Weisman GR, Wong EH, Rheingold AL, et al. Comparative in vivo stability of copper-64-labeled cross-bridged and conventional tetraazamacrocyclic complexes. J Med Chem 2004;47:1465–74.
[25] Sun X, Wuest M, Weisman GR, Wong EH, Reed DP, Boswell CA, et al. Radiolabeling and in vivo behavior of copper-64-labeled cross-bridged cyclam ligands. J Med Chem 2002;45:469–77.
[26] Wong EH, Weisman GR, Hill DC, Reed DP, Rogers ME, Condon JS, et al. Synthesis and characterization of cross-bridged cyclams and pendant-armed derivatives and structural studies of their copper(II) complexes. J Am Chem Soc 2000;122:10561–72.
[27] Sprague JE, Peng Y, Sun X, Weisman GR, Wong EH, Achilefu S, et al. Preparation and biological evaluation of copper-64-labeled tyr3-octreotate using a cross-bridged macrocyclic chelator. Clin Cancer Res 2004;10:8674–82.
[28] Wei LH, Butcher C, Miao YB, Gallazzi F, Quinn TP, Welch MJ, et al. Synthesis and biologic evaluation of Cu-64-labeled rhenium-cyclized alpha-MSH peptide analog using a cross-bridged cyclam chelator. J Nucl Med 2007;48:64–72.
[29] Geue RJ, Hambley TW, Harrowfield JM, Sargeson AM, Snow MR. Metal-ion encapsulation — cobalt cages derived from polyamines, formaldehyde, and nitromethane. J Am Chem Soc 1984;106:5478–88.
[30] Smith SV. Molecular imaging with copper-64. J Inorg Biochem 2004;98:1874–901.
[31] Di Bartolo NM, Sargeson AM, Donlevy TM, Smith SV. Synthesis of a new cage ligand, SarAr, and its complexation with selected transition metal ions for potential use in radioimaging. J Chem Soc-Dalton Trans 2001:2303–9.

[32] Bottomley GA, Clark IJ, Creaser II, Engelhardt LM, Geue RJ, Hagen KS, et al. The synthesis and structure of encapsulating ligands — properties of bicyclic hexamines. Aust J Chem 1994;47:143–79.
[33] Sargeson AM. The potential for the cage complexes in biology. Coord Chem Rev 1996;151:89–114.
[34] Voss SD, Smith SV, DiBartolo N, McIntosh LJ, Cyr EM, Bonab AA, et al. Positron emission tomography (PET) imaging of neuroblastoma and melanoma with 64Cu-SarAr immunoconjugates. Proc Natl Acad Sci U S A 2007;104:17489–93.
[35] Di Bartolo N, Sargeson AM, Smith SV. New Cu-64 PET imaging agents for personalised medicine and drug development using the hexa-aza cage, SarAr. Org Biomol Chem 2006;4:3350–7.
[36] Sprague JE, Kitaura H, Zou W, Ye Y, Achilefu S, Weilbaecher KN, et al. Noninvasive imaging of osteoclasts in parathyroid hormone-induced osteolysis using a 64Cu-labeled RGD peptide. J Nucl Med 2007;48:311–8.
[37] Haubner R, Wester HJ, Reuning U, Senekowitsch-Schmidtke R, Diefenbach B, Kessler H, et al. Radiolabeled αvβ3 integrin antagonists: a new class of tracers for tumor targeting. J Nucl Med 1999;40:1061–71.
[38] Haubner R, Bruchertseifer F, Bock M, Kessler H, Schwaiger M, Wester HJ. Synthesis and biological evaluation of a ^{99m}Tc-labelled cyclic RGD peptide for imaging the αvβ3 expression. Nuklearmedizin 2004; 43:26–32.
[39] Tai YC, Ruangma A, Rowland DJ, Siegel S, Newport DF, Chow PL, et al. Performance evaluation of the microPET Focus: a third-generation microPET scanner dedicated to animal imaging. J Nucl Med 2005;46:455–63.
[40] Cheresh DA, Spiro RC. Biosynthetic and functional properties of an Arg-Gly-Asp-directed receptor involved in human melanoma cell attachment to vitronectin, fibrinogen, and von Willebrand factor. J Biol Chem 1987;262:17703–11.
[41] Felding-Habermann B, Mueller BM, Romerdahl CA, Cheresh DA. Involvement of integrin alpha V gene expression in human melanoma tumorigenicity. J Clin Invest 1992;89:2018–22.
[42] Rogers BE, Anderson CJ, Connett JM, Guo LW, Edwards WB, Sherman ELC, et al. Comparison of four bifunctional chelates for radiolabeling monoclonal antibodies with copper radioisotopes: biodistribution and metabolism. Bioconjug Chem 1996;7:511–22.
[43] Bass LA, Wang M, Welch MJ, Anderson CJ. In vivo transchelation of copper-64 from TETA-octreotide to superoxide dismutase in rat liver. Bioconjug Chem 2000;11:527–32.
[44] Li WP, Meyer LA, Capretto DA, Sherman CD, Anderson CJ. Receptor-binding, biodistribution, and metabolism studies of Cu-64-DOTA-cetuximab, a PET-imaging agent for epidermal growth-factor receptor-positive tumors. Cancer Biother Radiopharm 2008;23: 158–71.
[45] Anderson CJ, Jones LA, Bass LA, Sherman ELC, McCarthy DW, Cutler PD, et al. Radiotherapy, toxicity and dosimetry of copper-64-TETA-octreotide in tumor-bearing rats. J Nucl Med 1998;39: 1944–51.
[46] McQuade P, Miao YB, Yoo J, Quinn TP, Welch MJ, Lewis JS. Imaging of melanoma using Cu-64- and Y-86-DOTA-ReCCMSH(Arg11), a cyclized peptide analogue of alpha-MSH. J Med Chem 2005;48: 2985–92.
[47] Weisman GR, Wong EH, Hill DC, Rogers ME, Reed DP, Calabrese JC. Synthesis and transition-metal complexes of new cross-bridged tetraamine ligands. Chem Commun 1996:947–8.
[48] Harrowfield JM, Herlt AJ, Lay PA, Sargeson AM, Bond AM, Mulac WA, et al. Synthesis and properties of macrobicyclic amine complexes of rhodium(III) and iridium(III). J Am Chem Soc 1983; 105:5503–5.
[49] Bernhardt PV, Bramley R, Engelhardt LM, Harrowfield JM, Hockless DCR, Korybutdaszkiewicz BR, et al. Copper(II) complexes of substituted macrobicyclic hexaamines — combined trigonal and tetragonal distortions. Inorg Chem 1995;34:3589–99.
[50] Comba P, Sargeson AM, Engelhardt LM, Harrowfield JM, White AH, Horn E, et al. Analysis of trigonal-prismatic and octahedral preferences in hexaamine cage complexes. Inorg Chem 1985;24:2325–7.
[51] Pfaff M, Tangemann K, Muller B, Gurrath M, Muller G, Kessler H, et al. Selective recognition of cyclic RGD peptides of NMR defined conformation by αIIbβ3, αvβ3, and α5β1 integrins. J Biol Chem 1994;269:20233–8.
[52] Haubner R, Gratias R, Diefenbach B, Goodman SL, Jonczyk A, Kessler H. Structural and functional aspects of RGD-containing cyclic pentapeptides as highly potent and selective integrin αvβ3 antagonists. J Am Chem Soc 1996;118:7461–72.
[53] Wu Y, Zhang XZ, Xiong ZM, Cheng Z, Fisher DR, Liu S, et al. microPET imaging of glioma integrin αvβ3 expression using Cu-64-labeled tetrameric RGD peptide. J Nucl Med 2005;46:1707–18.
[54] Haubner R, Wester HJ, Burkhart F, Senekowitsch-Schmidtke R, Weber W, Goodman SL, et al. Glycosylated RGD-containing peptides: tracer for tumor targeting and angiogenesis imaging with improved biokinetics. J Nucl Med 2001;42:326–36.